European Journal of Pharmaceutics and Biopharmaceutics 167 (2021) 104–113

Contents lists available at ScienceDirect

European Journal of Pharmaceutics and Biopharmaceutics

journal homepage: www.elsevier.com/locate/ejpb

Half-life extension of efficiently produced DARPin serum albumin fusions as a function of FcRn affinity and recycling

Hannes Merten [a], Fabian Brandl [a,b], Martina Zimmermann [a], Jonas V. Schaefer [a], Linda Irpinio [a], Kine M.K. Sand [c,d], Jeannette Nilsen [c,d], Jan Terje Andersen [c,d], Uwe Zangemeister-Wittke [a,b,*], Andreas Plückthun [a,*]

[a] Department of Biochemistry, University of Zurich, 8057 Zurich, Switzerland
[b] Institute of Pharmacology, University of Bern, Inselspital INO-F, 3010 Bern, Switzerland
[c] Department of Immunology, University of Oslo and Oslo University Hospital Rikshospitalet, N-0372 Oslo, Norway
[d] Institute of Clinical Medicine, Department of Pharmacology, University of Oslo, N-0318 Oslo, Norway

ARTICLE INFO

Keywords:
Serum albumin
FcRn
Half-life
HSA7
Pichia pastoris
Binding affinity
DARPin

ABSTRACT

Serum albumin shows slow clearance from circulation due to neonatal Fc receptor (FcRn)-mediated recycling and has been used for half-life extension. We report here fusions to a high-affinity DARPin, binding to Epithelial Cell Adhesion Molecule (EpCAM). We developed a novel, efficient expression system for such fusion proteins in *Pichia pastoris* with titers above 300 mg/L of lab-scale shake-flask culture. Since human serum albumin (HSA) does not bind to the murine FcRn, half-lives of therapeutic candidates are frequently measured in human FcRn transgenic mice, limiting useable tumor models. Additionally, serum albumins with extended half-life have been designed. We tested HSA7, motivated by its previously claimed extraordinarily long half-life in mice, which we could not confirm. Instead, we determined a half-life of only 29 h for HSA7, comparable to MSA. The fusion of HSA7 to a DARPin showed a similar half-life. To rationalize these findings, we measured binding kinetics and affinities to murine and human FcRn. Briefly, HSA7 showed affinity to murine FcRn only in the micromolar range, comparable to MSA to its cognate murine FcRn, and an affinity in the nanomolar range only to the human FcRn. This explains the comparable half-life of MSA and HSA7 in mice, while wild-type-HSA has a half-life of only 21 h, as it does not bind the murine FcRn and is not recycled. Thus, HSA-fusions with improved FcRn-affinity, such as HSA7, can be used for preclinical experiments in mice when FcRn transgenes cannot be used, as they reflect better the complex FcRn-mediated recycling and distribution mechanisms.

1. Introduction

Many therapeutic agents such as anti-cancer chemotherapeutics, cytokines or antibody fragments are small and thus rapidly cleared from the circulation by renal filtration, which hampers their efficacy [1]. To maintain long-lasting and efficacious blood levels upon administration, but avoid constant infusion or repeated injection, which is often associated with toxicity by the initially high peak levels, various half-life extension strategies have been explored. Most of those achieve half-life extension by simply increasing the size of drugs above the renal filtration threshold of 60–70 kDa [1]. A more sophisticated approach for half-life extension is to exploit the natural recycling and resorption mechanism of the neonatal Fc receptor (FcRn) by coupling, complexation or genetic fusion to human serum albumin (HSA) [2,3]. We report here fusions to a high-affinity targeting protein Designed Ankyrin Repeat Protein (DARPin), and the development of a powerful expression and purification system for such fusion proteins in *Pichia pastoris* with titers above 300 mg/L in lab-scale shake-flask cultures, making access to these fusion proteins very rapid and efficient.

Serum albumin is the most abundant blood protein and, with a concentration of 40 g/L (~600 μM), it constitutes 60% of the total plasma protein pool [3]. Nevertheless, two thirds of the serum albumin pool are circulating in the non-vascular space [3], e.g., the lymphatic system, saliva, the small intestine [4] and the fluid of the respiratory

* Corresponding authors at: Department of Biochemistry, University of Zurich, Winterthurerstrasse 190, CH-8057 Zurich, Switzerland (A. Plückthun), Department of Biochemistry, University of Zurich, Winterthurerstrasse 190, 8057 Zurich, Switzerland and Institute of Pharmacology, University of Bern, Inselspital INO-F, 3010 Bern, Switzerland (U. Zangemeister-Wittke).

E-mail addresses: uwe.zangemeister@pki.unibe.ch (U. Zangemeister-Wittke), plueckthun@bioc.uzh.ch (A. Plückthun).

https://doi.org/10.1016/j.ejpb.2021.07.011
Received 14 May 2021; Received in revised form 14 July 2021; Accepted 19 July 2021
Available online 23 July 2021

tract [5]. The mostly α-helical protein folds into the three homologous domains (DI, DII and DIII), and each is divided into an A and B subdomain and connected with flexible loops [6]. Its stable structure, high solubility, long half-life, biodegradability, and non-toxic and non-immunogenic nature, its easy availability, as well as its natural propensity to bind many different drugs, have motivated its use as carrier in drug development. Several HSA-based drugs have been approved for clinical use, such as the paclitaxel nanoparticle Abraxane® [3], direct HSA-fusion peptides or proteins like GLP-1-HSA [1] and factor IX-HSA [2], and more fusion proteins are in late-stage clinical trials.

Interestingly, serum albumin also seems to actively support drug delivery into solid tumors and the tumor microenvironment [7–10]. Although the main drivers are still unclear, various receptors including albondin (gp60) and secreted protein acidic and rich in cysteine (SPARC) are likely involved [3]. Other receptors also contribute to the complex transport and distribution of serum albumin. For instance, gp30 and gp18 are thought to perform a "quality control" and direct damaged or heavily modified serum albumin to lysosomal degradation, while megalin and cubulin mediate the reabsorption of serum albumin in the kidney [3].

However, the most prominent and best characterized serum albumin receptor is FcRn, which simultaneously also binds and regulates the trafficking and half-life of IgGs [2]. For IgGs, it was demonstrated that the complex with FcRn is internalized into acidified endosomes in endothelial cells by pinocytosis before it recycles back and releases the IgG into the blood due to its lower affinity at physiological pH (see below). A similar procedure can be expected for HSA.

HSA in humans has a half-life of 20 d [2]. Although in mice the half-life of mouse serum albumin (MSA) is only 30–35 h and thus much shorter than HSA in humans [11], it is also regulated by FcRn, since it was shown to decrease to about 20 h in mouse strains lacking a functional receptor [11]. Interestingly, this decrease was observed for both MSA and IgGs, although the respective native half-lives are largely different. In fact, FcRn is not only expressed in endothelial cells, but throughout many tissues and cells in the body, including cells of the immune system and the blood brain barrier, which contributes to the complex and broad biodistribution of serum albumin [2].

The FcRn consists of two chains, a 40 kDa α-chain with three extracellular domains (α1-α3), a transmembrane domain followed by a cytoplasmic tail of 44 amino acids, as well as a 12 kDa, non-covalently associated, β-chain (β_2m) [2]. Two complex structures for the human FcRn (hFcRn), either bound to wild-type (wt) HSA [12] or to a high-affinity version of HSA, selected by mutagenesis and yeast display (termed HSA13: V418M, T420A, E505G, V547A) [13]), provided detailed insight into the molecular mechanism of the HSA-FcRn interaction. It is a pH-controlled process, as the protonation of specific histidines at an acidic pH below 6 stabilizes a loop surrounding H166 in the α1-domain of FcRn, which carries key residues for the interaction, and the protonation of H510 and H535 in HSA results in a conformational change in a long loop connecting DIIIA and DIIIB. Subsequently, strong hydrophobic interactions of specific tryptophan residues of the FcRn with binding pockets in HSA, and a relative orientation shift of the subdomains mainly in DIII of HSA characterize the binding [12,13]. Schmidt et al. [13] proposed a model in which DIIIB is moving *after* initial binding, allowing full hydrophobic contacts of the W53-pocket.

Together with the available HSA-FcRn structure, another high-FcRn-affinity variant of HSA was reported, namely HSA7 (E505G, V547A), which carries only two of the four amino acid substitutions from HSA13 [13]. While the affinity of HSA13 to the human FcRn was even reported as a K_D of 8 nM at pH 6, the affinity of HSA7 was 64 nM under the same conditions. Importantly, it was claimed that its half-life was increased to 67.5 h in mice [13], being more than two times longer compared to that of MSA and longer than HSA13. These reports had motivated us to examine it as a fusion protein for half-life extension. Nonetheless, the biochemical rationale still had to be investigated, as the affinity of HSA7 to the murine FcRn (mFcRn) has not been determined yet.

A second high-affinity FcRn binder was engineered using knowledge-based design, and it was termed HSA^{K573P} [14]. An alignment of all known C-terminal amino acid sequences of albumin revealed that only human and orangutan serum albumin display a lysine at position 573, whereas all other species have a proline there. Consequently, when this lysine was mutated to proline, HSA^{K573P} showed strongly increased binding to the human FcRn (K_D: 61 nM), comparable to that of HSA7. However, its affinity to the murine FcRn remained much lower, in the range of the MSA binding (K_D of 1.6 and 0.8 μM respectively). This correlated with its half-life in mice, which was 30 h and, hence, again in the range of the MSA half-life [11]. Wt HSA, in contrast, was found to essentially not bind the murine FcRn [14–16]. Interestingly, the high human FcRn-affinity of the two published HSA variants cannot be easily explained from the reported structures [12–14], and there is increasing evidence that the murine FcRn binds serum albumins differently [13,16].

We were interested in investigating half-life extensions with such engineered HSA mutants for DARPins. DARPins represent a new class of non-IgG binding proteins that can have properties superior to antibodies in various biomedical applications, including tumor targeting. They are more stable than antibodies, have favorable biophysical properties, which increase their freedom of engineering into different formats, and they can be readily expressed in *E. coli* [17]. Nevertheless, due to their small size of usually less than 20 kDa, DARPins are rapidly cleared from the circulation, resulting in a half-life of only a few minutes [18,19]. We previously described the possibility to incorporate a single cysteine and a non-natural amino acid into the scaffold for PEGylation [18] or bio-orthogonal chemical coupling of a half-life extension module like serum albumin [19]. In addition, DARPins were fused to unstructured polypeptides of different lengths to optimize the half-life of these targeting molecules by controlling the apparent molecular weight [20].

Here, we investigated the potential of HSA7 for half-life extension of fusion proteins, originally motivated by the previous report of an extraordinary half-life in FcRn wt mice [13], and re-examined these values, determining the role of FcRn binding for the elimination kinetics in mice. To correlate these findings with biochemical data, we investigated the affinity of HSA7 for both the human and the murine FcRn using detailed SPR analyses. In this comparison, we used wt HSA, which does not bind to the murine FcRn, the high-affinity variant HSA7, and MSA.

To study the effect of FcRn binding on serum half-life, human FcRn transgenic mice can be used as an alternative [21]. However, this model has limitations, too, since the strong overexpression of the hFcRn itself leads to altered pharmacokinetic behavior of serum albumins, e.g., unnaturally long half-lives [13,14], which can result, e.g., in increased side-effects for specific drugs in these animals. Additionally, the transgenic human FcRn binds MSA still significantly, leading to a competition with the HSA-drug fusions [15]. Moreover, some disease models themselves require transgenes, and/or cannot be established in these mice.

To ensure facile production and sufficient material of HSA fusion proteins, we used *Pichia pastoris* [22,23], and developed a highly efficient expression system which allows high cell densities and protein titers as well as facile cultivation. Optimizing the *P. pastoris* strain, induction schemes, carbon source, and construct design, we arrived at a method and protocol which now allows to routinely obtain yields of 300 mg/L in standard laboratory shake flasks. HSA, HSA7 and the fusion proteins composed of HSA7 and the DARPin in different configurations could be purified from the cell culture supernatant using two consecutive orthogonal affinity chromatography steps. Altogether, this has now made the access to these fusion proteins very rapid and efficient.

Here, we correct the previously reported [13] very long half-life of HSA7 in wt mice. Instead, we find that the half-life of HSA7 is comparable to MSA, yet clearly longer than wt HSA. To correlate these findings with biochemical analyses, we report here surface plasmon resonance (SPR)-data showing that HSA7 binds to the murine FcRn with micromolar affinity, which is comparable to the murine FcRn-MSA

interaction. In contrast, HSA does not bind to murine FcRn but shows a high affinity to the human FcRn. Consequently, micromolar affinity to FcRn is the crucial minimal threshold for active *in vivo* recycling in mice.

Using a DARPin as an example, our data confirm the tremendous potential of the HSA7 expression platform to extend the half-life of small proteins in mice as a preferred preclinical model for drug testing. Since many favorable effects of serum albumins such as tissue penetration depend on an intact FcRn interaction, HSA7 offers the opportunity to exploit the FcRn-mediated transport pathways in mice and hence, in contrast to wt HSA, more closely mimics the clinical situation with HSA in humans.

2. Materials and methods

2.1. Cloning of serum albumins and HSA7-DARPin fusions for expression

For the production in *Pichia pastoris,* the expression constructs for human serum albumin (HSA) and HSA-DARPin fusions (HSA-FLAG, HSA7-FLAG, Ec1-HSA7-FLAG or HSA7-Ec1-FLAG) were based on the vector pPICZαA (Invitrogen). These configurations were chosen since the C-terminal FLAG does not interfere with the transport and leader sequences used for *P. pastoris* expression (see below), and fusing HSA7 to the EpCAM-binding DARPin Ec1 either N-terminally or C-terminally would allow us to identify the fusion protein with optimal expression properties and homogeneity (Fig. 1). The sequences of all constructs are shown in Figure S1. To optimize expression of these constructs, we investigated different versions of the α-mating factor (αMF) pre-pro transport region and the native serum albumin leader sequence. These constructs were generated with the same assembly strategy (see below) but using different synthetic nucleotide sequences in the assembly PCR step. We found that the best yields were obtained by the full-length α-mating factor transport region when using a newly developed expression protocol optimized for shake-flask scale (described below). We thus only list in detail here the optimized construct design (Figure S1) and the optimized protocol.

All optimized constructs contain the methanol-inducible alcohol oxidase (AOX1) promotor [24–26] at the 5′-terminus, the αMF sequence (including signal sequence, pro-region and the sequence EAEA), which is trimmed from the mature protein, followed by the first amino acids of HSA (DAHKSE). For the N-terminal DARPin fusion, the EAEA of αMF was followed by the amino acids DSGLD. The EpCAM-binding DARPin Ec1 [27] and the respective serum albumin (HSA or HSA7) were connected by a $(GGS)_4GG$ linker (both when N-terminally or C-terminally fused to serum albumin). At the C-terminal end of the ORF is a FLAG tag, and at the 3′-terminus of the gene the AOX1 transcription terminator.

The constructs were generated as described in the following. First, vectors containing HSA or HSA7 (containing the mutations E505G and V547A [13]) were obtained as a synthetic gene from Life Technologies. The vectors contained: a BsaI restriction site, the AOX1 promotor, the αMF secretion sequence, the HSA or HSA7 sequence, a FLAG tag and the AOX terminator followed by a BglII restriction site. The BsaI or BglII-complementary restriction sites BamHI or HindIII on the pPICZαA vector were used for the insertion of these constructs.

Second, for the generation of the DARPin fusions, PCR on the obtained vectors containing the synthetic sequences (Life Technologies) was performed to generate a first fragment. Either the HSA or HSA7 sequence followed by a FLAG tag, the AOX terminator and the BglII restriction site (N-terminal DARPin fusion), or the BsaI restriction site followed by the AOX1 promotor, the αMF secretion signal and the HSA or HSA7 (C-terminal DARPin fusion), were amplified. Third, an assembly PCR using short overlapping sequence stretches was performed with synthetic nucleotide sequences (Integrated DNA Technologies) containing either the BsaI site, AOX1 promotor, αMF secretion signal and a cloning cassette, which is flanked by BamHI and HindIII restriction sites followed by an encoded $(GGS)_4GG$ linker (N-terminal DARPin fusion), or the encoded $(GGS)_4GG$ linker followed by the described cloning cassette, a FLAG tag, the AOX1 terminator and a BglII restriction site (C-terminal DARPin fusion). The generated full-length construct PCR fragments were cloned into pPICZαA using again BsaI and BglII and the complementary restrictions sites BamHI and HindIII on the vector. In a last step, the described cloning cassette was exchanged by the DARPin Ec1 [27] using the 5′ BamHI and 3′ HindIII restriction sites.

2.2. Protein expression in Pichia pastoris

All media were sterile-filtered and methanol was added afterwards.

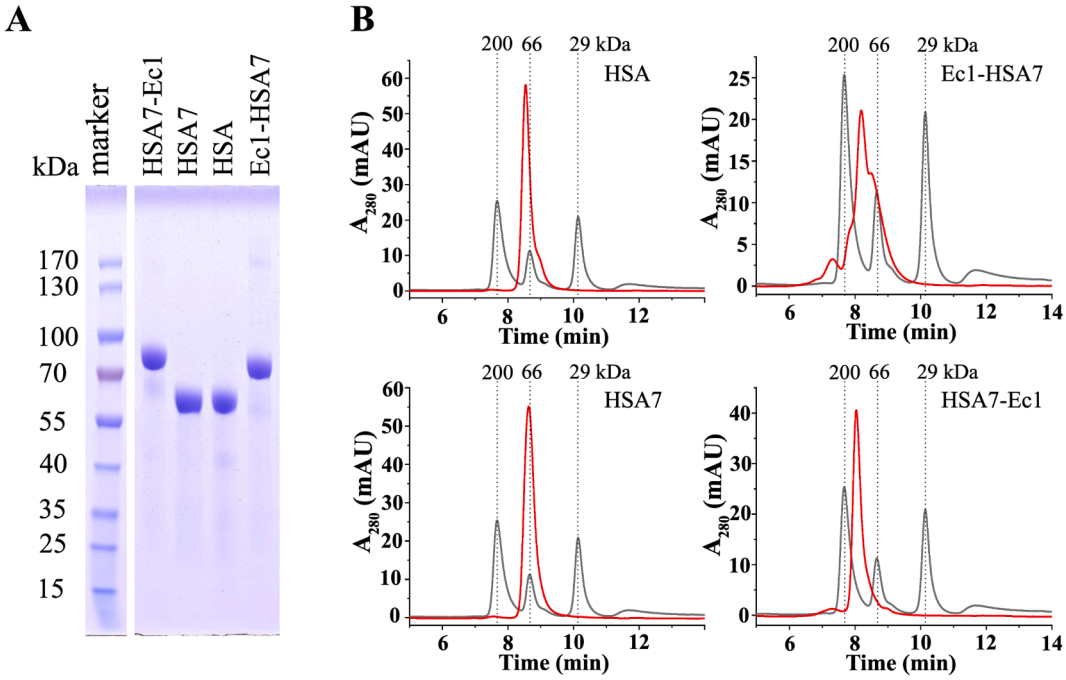

Fig. 1. Analysis of purified HSA variants and DARPin fusions after expression in *P. pastoris*. A) SDS-PAGE gel analysis. B) Analytical gel filtration for apparent molecular size and homogeneity analysis; red: sample chromatogram; light grey: protein standard chromatogram.

All steps with cells were performed under sterile conditions. The vectors containing the αMF-HSA-FLAG, αMF-HSA7-FLAG, αMF-Ec1-HSA7-FLAG or αMF-HSA7-Ec1-FLAG construct were linearized using the BglII site (in front of the AOX promotor). The linearized plasmid was purified with isopropanol precipitation, and electrocompetent SMD1163 (*his4 pep4 prb1*, phenotype His$^-$) or KM71H (*aox1::ARG4, arg4*, phenotype Mut^S) cells (Invitrogen) were transformed with the linearized plasmid. Forty microliters of cells were mixed with 400 ng of linearized plasmid DNA and the whole mix was plated after electroporation with 1500 V (Eppendorf Electroporator 2510) on YPD-Agar (Formedium) plates (containing 100 μg/mL Zeocin™) following standard procedures [28]. After 3–4 days of incubation at 30°C, single colonies were re-plated on fresh YDP-agar (100 μg/mL Zeocin™).

A pre-culture of 5 mL YPD medium (Formedium) was inoculated from a single colony and incubated for 18 h at 30°C with continuous shaking. Thereafter, 5 mL BMMY medium (1% (w/v) yeast extract, 2% (w/v) peptone, 100 mM potassium phosphate pH 6.0, 1.34% (w/v) yeast nitrogen base (YNB, w/o amino acids), 0.5% (v/v) methanol, 0.04% (w/v) biotin) were inoculated to an OD_{600} of 1.0, and the cells were grown for 24 h at 30°C with continuous shaking in the expression medium. Finally, the cell suspension was centrifuged for 5 min at 1500 × g, and the supernatant was separated from the pellet.

To monitor expression yields and determine product integrity, the C-terminal FLAG-tag was detected by dot blotting. Four microliters of supernatant were added to a nitrocellulose membrane (Whatman) and the membrane was dried for 10 min at 37°C. This step was repeated two times and the membrane subsequently blocked with PBS-TM-5 (PBS, 0.05% (v/v) TWEEN®-20, 5% (w/v) non-fat milk powder (AppliChem)), incubated with the monoclonal mouse anti-FLAG M2 antibody (Sigma Aldrich, F3165) in PBS-TM-2.5 (PBS, 0.05% TWEEN®-20, 2.5% (w/v) non-fat milk powder) and washed 4 times with PBS-T (PBS pH 7.4, 0.05% TWEEN®-20) for 5 min before incubating it with the goat anti-mouse IgG-AP conjugate (Sigma Aldrich, A3562) in PBS-TM-2.5 (PBS, 0.05% TWEEN®-20, 2.5% (w/v) non-fat milk powder) and washing it again as before. All blocking and incubation steps were performed for 1 h at room temperature.

The membrane was developed using BCIP®-NBT solution (Sigma Aldrich) and, when spots became clearly visible, the development was stopped with a single wash step with PBS-T for 5 min. For each construct in each strain, 10–15 clones were tested, and the supernatant of well-performing clones was also analyzed by SDS-PAGE.

The best-performing clones were used for the inoculation of 5 mL YPD medium and grown for 18 h at 30°C with continuous shaking. After centrifugation, the cell pellet was resuspended in 1 mL fresh YPD medium containing 20% (v/v) glycerol, the cells were gradually frozen using an isopropanol freezing container (Thermo Fisher Scientific) and stored at −80°C for conservation.

For lab-scale expression (0.5 L), previously conserved cells of a selected clone were re-streaked on a YPD-Agar plate (containing 100 μg/mL Zeocin™) and after 2–3 days of incubation at 30 °C two 100 mL pre-cultures in YPD medium in unbaffled 1 L shake flasks were inoculated from a single colony and grown under continuous shaking (125 rpm, ø 25 mm) overnight. The next day, 0.5 L BMMSY expression medium (1% (w/v) yeast extract, 2% (w/v) peptone, 100 mM potassium phosphate pH 6.0, 1.34% (w/v) YNB (w/o amino acids), 2% (v/v) methanol, 0.04% (w/v) biotin), 1% (v/v) sorbitol) in 2.5 L Ultra Yield™ flasks (THOMSON instrument company, #931136B) was inoculated to an OD_{600} of 1.0 with the pre-cultures. A minimal pre-culture dilution factor of 1:25 was used to avoid high glucose concentrations from residual YPD medium in the expression culture. Ninety microliters antifoam 204 (Sigma Aldrich) were added, the flasks sealed with AirOtop™ lids (THOMSON instrument company, #899425) and the expression culture was incubated at 30 °C for 72 h under continuous shaking (300 rpm, ø 25 mm). Two percent (v/v) methanol was added every 24 h. Expression cultures were centrifuged at 1500 × g for 10 min and the supernatant harvested and sterile filtered (VacuCap® PF bottle-top filter device, PALL) and stored at 4 °C prior to protein purification. Note that above, the final expression protocol is described, whereas throughout optimization different methanol feeding concentrations, glycerol instead of sorbitol, and an expression without glycerol or sorbitol were all tested.

2.3. Purification of serum albumins and HSA7-DARPin fusions from the supernatant

All purification steps were performed using an ÄKTA™ Pure chromatography system (GE healthcare). The filtered supernatants (500–1000 mL) were loaded to a 20 mL glass-shell self-packed AlbuPure (Prometic Bioseparations) resin column. Briefly, the column was equilibrated with 5 column volumes (CV) equilibration buffer (50 mM sodium citrate, pH 5.5), the supernatant loaded with a minimal contact time of 4 min, and the column washed with 5 CV equilibration buffer followed by 5 CV wash buffer 1 (50 mM sodium phosphate, pH 6.0) and 10 CV wash buffer 2 (50 mM sodium citrate). Ten CV elution buffer (50 mM ammonium acetate, 100 mM sodium octanoate, pH 7.0) were applied and protein-containing fractions (280 nm absorbance) collected and pooled. All AlbuPure-steps were run with a flow rate of 5 mL/min. To remove aggregates, the collected protein pools were loaded to a strong anion exchange MonoQ 5/50 GL column (GE healthcare). After equilibration with 20 mM HEPES, 20 mM NaCl, pH 8, the protein pool was loaded with a contact time of 4 min, the column washed with 10 CV equilibration buffer and the protein eluted with a linear gradient of 10–50% 20 mM HEPES, 1 M NaCl, pH 8 over 50 CV with a contact time of 4 min. Protein-containing fractions (280 nm absorption) were collected, dialyzed against PBS and pooled.

2.4. Endotoxin removal

For endotoxin removal, purified proteins were applied to an EndoTrap HD affinity resin according to the manufacturer's instructions (Hyglos, product discontinued, now marketed by Lionex GmbH, Braunschweig). Proteins were buffer-exchanged to endotoxin-free Dulbecco's PBS (Millipore) using PD-10 desalting columns (GE Healthcare). The endotoxin content was determined after 1:40 dilution in glucan blocking buffer (Charles River Laboratories, BG120) with an EndoSafe Portable Test System (Charles River Laboratories) using PTS test cartridges (Charles River Laboratories) with 0.5–0.005 EU/mL sensitivity. In all purified samples, the amount of detected endotoxin was always below 0.7 EU/ml or 1.3 EU/mg of protein.

2.5. SDS-PAGE analysis

Two micrograms of protein were analyzed by SDS-PAGE using 4–12% ExpressPlus™ PAGE Gels (GenScript) with MOPS SDS running buffer (GenScript) according to the manufacturer's instructions. As molecular weight standard PageRuler™ Prestained Protein Ladder (Thermo Fisher Scientific) was used. Gels were stained according to the manufacturer's instructions with Coomassie Brilliant Blue R250 (Sigma-Aldrich).

2.6. Analytical gel filtration

Proteins were analyzed on an Agilent Advanced BioSEC column (300 Å, 2.7 μm, 4.6 × 300 mm, Agilent) connected to an Agilent 1260 Infinity Bio-inert Quaternary LC HPLC system (Agilent). Ten microliters of protein dilutions in PBS pH 7.4 were injected into the HPLC system at a flow rate of 0.35 mL/min. The elution profiles were monitored by absorbance at 280 nm. A molecular weight gel filtration standard (Agilent) was included.

2.7. Binding kinetics by surface plasmon resonance

The binding kinetics of serum albumins or serum albumin-DARPin

fusions to FcRn were determined on a ProteOn™ XPR36 instrument (BioRad). Human or murine FcRn fusions with glutathione-S-transferase (FcRn-GST) were expressed and purified as previously described [29,30]. FcRn-GST was biotinylated using NHS-LC-LC-Biotin (Thermo Fisher Scientific) dissolved in DMSO. Briefly, the proteins were incubated with 8 × molar excess of NHS-linker for 2 h on ice and thoroughly desalted (ZebaSpin column, Thermo Fisher) using PBS buffer. To assess the degree of biotinylation, the desalted proteins were mixed with commercially available streptavidin (1.2 g/L in PBS) in 2 × molar excess, incubated for 1–2 h at 24 °C and analyzed on an SDS-PAGE gel. Two ligand channels of a NeutrAvidin-functionalized chip (ProteOn™ NLC Sensor Chip, BioRad) were coated with biotinylated FcRn-GST in PBS-T (PBS pH 7.4, 0.005% TWEEN®-20) in a high or low density. For each ligand/analyte pair, coating densities were optimized, reaching minimally 500 RU (low density) and maximally 1200 RU (high density). After coating, the running buffer was changed to PBS-T pH 6.0. After three buffer injections for baseline stabilization, a 1:1.85 dilution series of analyte was injected, starting with optimized concentrations for each construct of 1.34 μM (HSA7-Ec1), 13.73 μM (HSA7) or 5.97 μM (MSA) on the high- or low-density ligand channels. The flow rate of all steps was 60 μL/min, the association time was set to 250 s and the dissociation time to 800 s. The chip surface coated with FcRn-GST ligand was regenerated between analyte runs by a single PBS-T pH 7.4 injection with a flow rate of 60 μL/min and a contact time of 200 s. Data and assay quality was assured by verifying that buffer injections over coated channels or analyte (serum albumin) injections over uncoated channels did not show significant binding signals. The sensorgrams of analyte injections at a concentration giving a sufficient signal-to-noise ratio, but no non-specific chip surface binding, were double-referenced by subtraction of inter-spot signals and a blank analyte channel signal. The parameters of a 1:1 Langmuir binding model, or in the case of MSA/mFcRn a heterogeneous ligand model, were fit to the data using the ProteOn™ Manager Software (Version 3.1.0.6, BioRad).

2.8. Mice

Female Crl:CD1-*Foxn*1^{nu} mice 6–8 weeks of age were purchased from Charles River Laboratories and kept under sterile conditions according to the guidelines of the veterinary ordinance of the Kanton Zurich for animal welfare.

2.9. Pharmacokinetic analysis – Blood clearance in mice

To determine the blood clearance kinetics of HSA, HSA7 and the HSA7-Ec1 fusion protein, mice were injected intravenously (i.v.) into the tail vein with 4 mg/kg of protein (N = 5 mice per group). This represents a typical dose for the pharmacokinetic characterization of proteins in this half-life range [13,14,20], which results, in a first approximation, in serum protein levels that can be well detected by ELISA. Only constructs showing high homogeneity were selected for *in vivo* experiments (Fig. 1A, B). Blood samples were drawn from the saphenous vein after 3 min, 1, 8, 24, 48, 72 and 96 h. After blood coagulation at room temperature for 30 min, serum was prepared by two centrifugation steps (coagulated blood 7 min at 3100 × g, serum 3 min 5000 × g, room temperature) and stored at − 80 °C until quantification of serum concentrations by a carefully calibrated pull-down sandwich ELISA.

Black 384-well Immuno Plates (Thermo Fischer Scientific) were coated with 20 μL mouse anti-FLAG-M2 antibody (Sigma Aldrich, F3165) at a dilution of 1:500 in PBS pH 7.4 at 4°C overnight. The wells were blocked for 1 h at room temperature with 70 μL PBS-TM-4 (PBS pH 7.4, 0.05% TWEEN®-20, 4% w/v nonfat dried milk powder (AppliChem)). The wells were washed three times with 100 μL PBS-T (PBS pH 7.4, 0.05% TWEEN®-20) at room temperature using a plate-washing device (BioTEK Instruments). For the quantification of serum concentrations, a serial dilution of purified serum albumins or serum albumin-DARPin fusion in PBS-TM-4 was prepared, ranging from 125 to 0.12 nM. The PBS-TM-4 was supplemented with serum from an untreated animal in a 1:50 dilution to ensure an identical composition of the sample matrix. Twenty microliters of the diluted serum samples (1:50 in PBS-TM-4) or the standard dilution series were applied to the previously coated and blocked wells. Control wells were incubated with PBS-TM-4 without serum albumin or mouse serum for background subtraction. Furthermore, for assay quality assessment, the highest standard curve concentration of the purified protein without mouse serum, wells without solution, and wells with PBS-TM-4 without any protein or coating, were measured on the same plate. The plate was incubated for 1 h at room temperature, washed three times with PBS-T as above and incubated for 1 h at room temperature with 20 μL of a 1:4000 dilution of a mouse monoclonal anti-human serum albumin HRP antibody (AbCam, ab24458) in PBS-TM-4. After four final washing steps with PBS-T as above, the assay was developed using Amplex UltraRed (Thermo Fisher Scientific). A 10 mM Amplex UltraRed solution in DMSO was diluted 1:400 in 75 mM Na-citrate pH 6.0, 0.0035% (w/w) H_2O_2 and 20 μL were added to each well for detection. Fluorescence was measured every three minutes using a BioTek Synergy HT plate reader (BioTek Instruments). Following each solution addition to the wells in the protocol, plates were centrifuged for 1 min at 1500 × g and all incubation steps were conducted in a temperature-controlled environment.

All standards were prepared in triplicates ($N = 3$) and each data point was measured in quadruplicates ($N = 4$). The signal over time for the assay development of the highest concentration of the standard dilutions was plotted, and a read in the linear range of the signal development curve was selected (usually 6–12 min after dye addition). Non-linear regression using a 4PL-model was used to fit the data from serial standard dilutions to obtain a standard curve (Graph Pad Prism Version 6.07, GraphPad Software Inc.). Protein concentrations in the serum samples were quantified by interpolation of measured data points with the respective standard curve.

Data fitting and calculation of pharmacokinetic parameters with a two-compartment model (2-phase exponential decay) was performed using GraphPad Prism 6 (Version 6.07, GraphPad Software Inc.). The area under the curve (AUC) was calculated by integration of the two-compartment model curves, describing the distribution and elimination of the various i.v. injected serum albumins and DARPin-fusions. Clearance (CL), elimination rate constant (k_e) and apparent volume of distribution (V_d) were calculated with the formulas: $CL = D/AUC$, $k_e = \ln(2)/\tau^{\beta}_{1/2}$, $V_d = CL/k_e$, where D is the dose and $\tau^{\beta}_{1/2}$ is the terminal half-life.

3. Results

3.1. Production of serum albumins and DARPin-fusions in Pichia pastoris at high yield and purity

We developed a method that allowed us to express serum albumins and their fusion proteins in *P. pastoris* with a titer of > 300 mg/L in simple shake flasks. We typically used 0.5 L medium in 2.5-L flasks. We achieved this high yield by combining four components, (i) the use of the strain KM71H, which is not protease-deficient, (ii) an optimized methanol feeding plan and time course, (iii) the non-promotor-inhibiting carbon source sorbitol and (iv) shake flasks with a specific baffle design.

When developing this expression strategy, we measured the methanol content of the expression medium over time with 1D H-NMR (methanol peak integration) and found that it was massively consumed in the growth phase, because methanol serves as carbon source via the alcohol oxidase pathway, in addition to inducing the AOX promotor (data not shown). Consequently, a refeeding schedule was designed to keep the methanol level constant at 2% (v/v) throughout the growth phase. We therefore refute the widespread belief that methanol is toxic to *P. pastoris* [31], since in the saturation phase we measured methanol levels of > 5% (v/v), with no signs of toxicity to the cells, which would

be manifested, e.g., by a decrease in OD_{600}. We added sorbitol to the expression medium at the beginning, as it is a carbon source that does not inhibit the AOX promotor. While it neither increased the expression yield nor the cell density by itself, it decreased the required expression time, compared to an AOX-promoter-inhibiting carbon source like glycerol, as methanol can only induce the AOX promotor *after* the inhibiting carbon source is consumed. Therefore, the presence of sorbitol resulted in a better protein quality (lower protease-mediated degradation in the medium). Without an additional carbon source in the expression medium, cell densities and expression yields were significantly lower.

Frequently, the protease-deficient strain SMD1163 is used for secreted proteins. However, we found that this designed sorbitol and methanol feeding schedule applied to clones of the strain KM71H, which is not protease-deficient, greatly increased the protein yields by a factor of 5–10, compared to SMD1163.

Finally, the expression in UltraYield™ flasks enabled a filling volume of 0.5 L in a 2.5 L shake flask, while in a conventional 1 L shake flask the maximum filling volume can only be 100 mL without decreasing the cell growth and protein yield by diminished aeration.

Using this optimized expression strategy, HSA, HSA7 and the fusion proteins composed of HSA7 and the DARPin Ec1 in different configurations were purified from the *P. pastoris* cell culture supernatant with two consecutive orthogonal affinity chromatography steps, using first an AlbuPure® and second an anion exchange column, which resulted in protein preparations of high purity (Fig. 1A).

The anion exchange step minimized the aggregate and dimer content of all protein pools; however, the N-terminal fusion of the DARPin Ec1 showed lower homogeneity (Fig. 1B), as detected by analytical gel filtration analysis. It was therefore excluded from further characterization.

3.2. HSA7 has very different affinities for the human and the murine FcRn

The purified HSA-constructs and commercially obtained MSA (Merck Millipore) were tested by surface plasmon resonance (SPR) at pH 6.0 to determine the precise affinity parameters for the human and the murine FcRn. Both high- and low-density coated ligand channels resulted in comparable affinity parameters for each protein, and the fits follow well the sensorgram data (Fig. 2). This allows a precise and profound characterization of FcRn-binding behavior in a comprehensive dataset, consistent with SPR-data representation guidelines, as described in [32,33]. All examined analyte/ligand combinations could be thoroughly regenerated with a single PBS pH 7.4 injection, showing no residual binding at this pH.

The tested HSA7 showed high-affinity K_D values (Table 1) for the human FcRn, which compare well with data from the literature [13], and it confirms that there is no functional difference between the proteins produced in *Pichia pastoris* or *Saccharomyces cerevisiae*. Importantly, the C-terminal fusion of a DARPin (Ec1) to HSA7 did not mitigate the binding to the FcRn (Table 1).

We measured here for the first time also the affinity of the previously reported high-FcRn-affinity HSA variant HSA7 for the murine FcRn and found that it was strongly decreased, about 60-fold, compared to the human FcRn. As expected, HSA did not bind to the murine FcRn (Figure S2). Importantly, the determined affinities for the murine FcRn for HSA7 or its C-terminal DARPin fusion are thus in the same single-digit micromolar range as for MSA binding to its natural recycling receptor.

MSA binds to the human FcRn with affinities comparable to previously published data [15], but, interestingly, shows a different binding behavior to the human or murine receptor. The interactions with the human FcRn correspond to a simple 1:1 binding interaction and could be

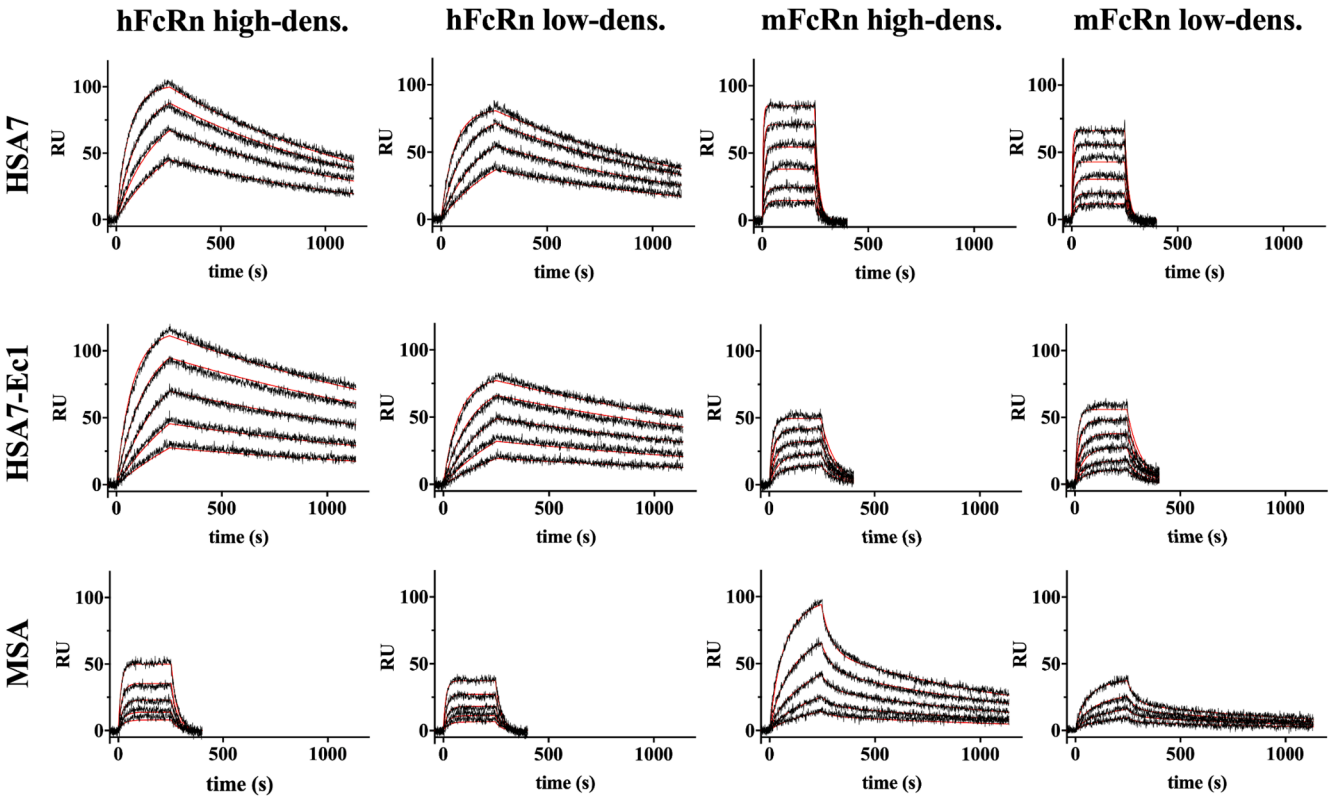

Fig. 2. SPR analysis of the binding kinetics of HSA7, HSA7-Ec1 and MSA to the human and murine FcRn. A 1:1 Langmuir model or heterogeneous ligand model were fit to the resulting sensorgrams, and kinetic parameters k_a, k_d and K_D were determined for each interaction. Measured signals are shown in black, fits are shown in red. *high-dens.*, high coating density of immobilized biotinylated FcRn-GST, low-dens., low coating density (cf. Section 2.7.). RU, resonance units.

Table 1
Affinity parameters at pH 6.0 for the tested HSA7, MSA and HSA7-Ec1/FcRn pairs.

Construct	FcRn species	k_a ($\times 10^3$ $M^{-1}s^{-1}$)	k_d ($\times 10^{-3}$ s^{-1})	K_D (nM)
HSA7	human	13.3; *13.4*	0.95; *0.87*	72; *65*
HSA7-Ec1	human	33.3; *34.0*	0.5; *0.5*	15.2; *14.5*
MSA	human	6.5; *7.8*	3.7; *3.6*	5700; *4600*
HSA7	murine	13.6; *15.1*	56.5; *60.3*	4200; *4000*
HSA7-Ec1	murine	39.0; *44.2*	14.6; *14.5*	374; 330
MSA	murine	1.5, 0.6; *1.5, 1.1*	0.9, 22.4; *1.0, 26.7*	599, 39990; *661, 24000*

k_a, association rate constant; k_d, dissociation rate constant; K_D equilibrium dissociation constant. Binding to MSA is shown for comparison. Plain text: high-density channel values, *italics*: low-density channel values. Note that a heterogeneous ligand model was fit to the MSA/mFcRn data, implicating two sets of parameters for each density. HSA does not bind to the murine FcRn (Figure S2), and numerous studies showed an approximately single-digit micromolar affinity to the human FcRn [13–16,44,52].

well fit with the 1:1 Langmuir model. However, the binding of MSA to the murine FcRn follows different, non-1:1 binding kinetics and requires a heterogeneous ligand binding model. The applied binding model generated a second set of parameters for these interactions, suggesting a second type of ligand/analyte interaction at pH 6, at which all the measurements were performed. This second interaction has increased dissociation rate constants, whereas the association rate constants are comparable, also to the human FcRn binding (Table 1). From these results, we conclude that there is a distinct binding mode of MSA to its natural murine FcRn, due to two different conformations at pH 6, which allow slow or fast MSA dissociation, possibly by a conformational change in the receptor which facilitates dissociation.

3.3. Binding to the murine FcRn increases the half-life of HSA in mice

The sandwich ELISA established in this work allows the precise and robust measurement of very low HSA concentrations down to 0.2 nM in the serum, with an excellent signal-to-noise ratio, and thus it enabled us to reliably determine the blood clearance curves of HSA, HSA7 and HSA7-Ec1 (Fig. 3).

As shown in Table 2, analyses of the curves and calculation of the underlying pharmacokinetic parameters revealed the fastest clearance

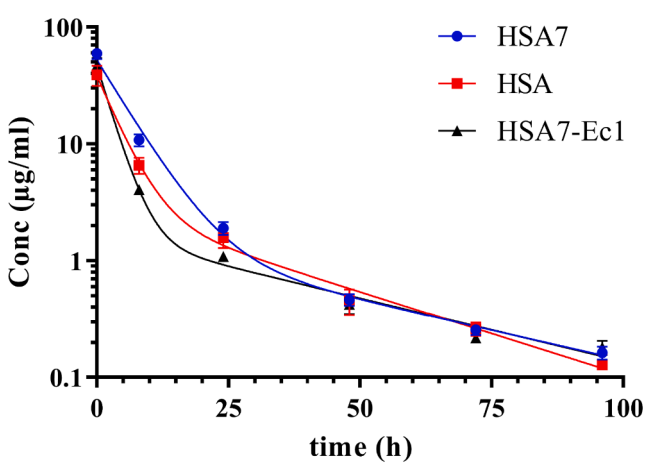

Fig. 3. Blood clearance of HSA, HSA7 and its fusion to the DARPin Ec1 in mice. All proteins were injected i.v. into mice at 4 mg/kg (N = 5 mice per group). Blood samples were collected 3 min, 1, 8, 24, 48, 72 and 96 h after injection. The serum concentrations were quantified by sandwich ELISA and interpolation with an appropriate protein standard. Data points are the average ± SD of N = 4–5 mice. A two-compartment model (bi-exponential decay) was fit to the data using GraphPad Prism version 6.07.

Table 2
Pharmacokinetic parameters of HSA, HSA7 and HSA7-Ec1 in mice.

Construct	$\tau^{\beta}_{1/2}$ (h)	AUC (h µg ml^{-1})	CL (ml h^{-1})	k_e (h^{-1})	V_d (ml)
HSA	21	283.9	0.409	0.033	12.4
HSA7	29	422.9	0.246	0.024	10.3
HSA7-Ec1	28	274.1	0.379	0.025	15.1

The values were calculated from the blood clearance curves shown in Fig. 3. $\tau^{\beta}_{1/2}$: terminal serum elimination half-life; AUC: area under the curve; CL: clearance rate; k_e: elimination rate constant; V_d: apparent volume of distribution. For comparison, the half-life of MSA was determined to be 30–35 h [11]

and elimination rate for HSA in mice, resulting in a half-life of 21 h. For HSA7, showing similar micromolar affinity to murine FcRn as MSA, we determined a half-life of 29 h. This is substantially shorter than the 67.5 h previously reported [13], which had motivated us choosing this variant, yet the published value is not even well supported by the published data points shown in Figure 6A in [13] (see Discussion). The C-terminal DARPin fusion, HSA7-Ec1, showed a similar half-life as HSA7. This demonstrates the potential of HSA7 to substantially increase the short half-life of a DARPin from a few minutes [18,19] to more than one day and shows that the elimination kinetics are determined by HSA7.

The determined half-lives of HSA7 and HSA7-Ec1 were thus comparable to those of MSA in its natural environment, in the blood circulation of wt mice [11]. This is well consistent with the similar low micromolar affinity of these proteins to the murine FcRn. In contrast, HSA, which does not bind to the murine receptor, revealed a significantly shorter half-life of 21 h. These data match and complement well the half-life values and murine FcRn binding parameters of HSA^{K573P}, another high-affinity FcRn-binding variant of HSA [14].

Table 2 further shows that the investigated proteins have high apparent distribution volumes in the range of the calculated total body fluid of mice [34], which can be expected from the high extravasation and tissue penetration capacity of HSA.

All observed AUC values are comparable between the investigated proteins, because the major part of the AUC value for serum albumins is influenced by the alpha distribution phase. Because the FcRn is highly saturated *in vivo*, recycling does not play a significant role in this phase and, consequently, all proteins examined are similarly distributed.

4. Discussion

We wished to investigate whether high-affinity variants of HSA can extend the half-life of binding proteins such as DARPins in wt mice, in order to have a greater freedom in the subsequent use of different disease models. For this reason, we developed first a highly efficient method of producing such fusion proteins in *P. pastoris*, and then established to what extent such high-affinity variants do increase the half-life and how this is correlated to the affinity to murine and human FcRn, compared to MSA and wt HSA.

4.1. Optimization of the Pichia expression system

To produce HSA, HSA7 and the DARPin-HSA7 fusion proteins at high quality and quantity, we established a facile production process for the high-yield protein expression in *P. pastoris* in a 0.5 L volume scale in shake flasks with titers of 300 mL/L, without the need for specific equipment. Using the designed vectors, we demonstrate that any DARPin can be readily fused to HSA or HSA7 and is secreted to the culture medium.

While the protease-deficient strain SMD1163 is frequently used for production of secreted proteins [23], the strain KM71H, which is not protease-deficient, increased the yield 5 to 10-fold over SMD1163. We conclude that the yield-limiting process is not the degradation of serum albumin in the cell culture supernatant by yeast proteases (e.g., released by disintegrated cells), but the decreased fitness of the protease-deficient

cells. PEP4, one of the deleted genes in SMD1163, encodes an aspartyl protease and such enzymes are involved in the vacuolar disposal of cellular debris arising from reactive oxygen species of the methanol metabolization pathway [35]. The other silenced gene, PRB1, also codes for a vacuolar protease (vacuolar proteinase B, [23]) and, hence, might play a similar role in this process. Consequently, we hypothesize that the protease-deficient strain SMD1163 is unable to process the high amounts of intracellular debris, which may be particularly abundant in high-density expression cultures protocols with high methanol concentrations.

To rule out other reasons for the higher yield from strain KM71H, we also determined the gene copy number in selected clones by qPCR. We found no increased copy number over SMD1163 (Table S1) and, hence, concluded that the above discussed strain-fitness was mainly influencing protein expression. In addition, different leader sequences (e.g., HSA leader) were tested, but no significant influence on the protein titer or quality was detected (data not shown).

Another component significantly increasing the protein yield was the elevated methanol concentration in our protocol, compared to commonly recommended procedures using the alcohol oxidase (AOX) promotor [24–26]. It has often been stated that methanol and its metabolic products are toxic to the *Pichia* cells [31], and this statement is often repeated by numerous online protocols from suppliers, yet without mentioning a tangible toxicity level, but instead recommending very low methanol levels of 0.5–2.0% (v/v). Thus, in standard protocols, methanol is added only once at the very beginning of the cultivation, supposedly providing sufficient levels for both growth *and* recombinant protein production with the AOX promotors. However, the cells are well protected from the reactive oxygen species products of the methanol metabolites H_2O_2 and formaldehyde [36]. These protection mechanisms include, amongst others, the oxidation of essential thiol groups in the AOX enzyme by H_2O_2 if this toxic substance is present in high amounts and cannot be neutralized by other protective pathways [26]. This thiol oxidation inactivates the AOX enzyme and thus methanol utilization ceases and, as a consequence, H_2O_2 production also stops, which would have resulted in reduced growth rates. Nevertheless, apoptosis or uncontrolled cell death are avoided by this protective mechanism. Consequently, until decreased growth-rates are detected, we found that methanol feeding can be increased for every lab-scale cultivation experiment.

Furthermore, we used sorbitol as additional carbon source which, in contrast to glucose or glycerol [37–39], is not repressing the AOX promotor [40]. While sorbitol has been applied in fermenter-scale cultivation experiments [41,42], we provide here for the first time a protocol for shake flask cultures.

The yeast-expressed proteins showed a good quality, except for the N-terminal DARPin fusion of HSA7, Ec1-HSA7, which revealed an increased aggregate content (Fig. 1) and major deviations in analytical SEC from the calculated mass (data not shown). We hypothesize that the extremely fast and stable folding of the DARPin [17] might overstrain the export and folding control apparatus of the yeast cells, an effect which was previously observed in bacteria [43], and that this occurs already during expression, as all proteins were found to be stable

4.2. Relation of half-life and binding to murine FcRn

HSA7 is characterized by a strongly increased affinity to the human FcRn compared to HSA [13]. Whereas HSA does not effectively bind to the murine FcRn, the affinity of HSA7 to it had not been investigated yet, and it seemed plausible that HSA7 not only binds better to human FcRn but also to murine FcRn. Therefore, fusions to HSA7 might be a better model of half-life extension in wt mice than fusions to HSA, which does not undergo FcRn-dependent recycling in mice, for disease models where hFcRn transgenic mice cannot be used. Moreover, fusions to HSA7 might be moved to the clinic in a more straightforward way than fusions to MSA. We determined the affinity of HSA7 to murine FcRn to be in the micromolar range, and in mice its half-life was shown in the presented study to be 29 h, compared to only 21 h for HSA. Thus, HSA7 equals the half-life of MSA in mice [11]. The presented study completes the picture of data collected with MSA [11] and HSA^{K573P} [14]. Because all these proteins bind to the murine FcRn with a micromolar affinity, they consequently all show a half-life around 30 h in mice. Interestingly, the half-life-engineered HSA variants reach this value, even though they compete with an enormous excess of circulating MSA in the blood stream. Importantly, the exceedingly long half-life of HSA7 previously reported [13] could not be confirmed, and the published data points (cf. Figure 6A in [13]) would actually be more consistent with the rates determined here and for HSA^{K573P} [14], as well as those for MSA itself [11]. Consequently, the provided more complete picture of the relationship between half-life and FcRn binding should be taken into account in preclinical drug testing, specifically because FcRn-mediated transport affects the biodistribution of the HSA-fused drug.

Other receptors which may affect the tissue distribution and half-life of HSA variants *in vivo* include binding to albondin (gp60), SPARC, gp18, gp30 and the megalin-cubulin complex [3]. These interactions may also deplete the pool of circulating HSA, e.g., by receptor-mediated clearance. However, in contrast to FcRn binding, the effect of these interactions can be considered equal for both HSA variants. Our wt mouse model to investigate the pharmacokinetic properties of HSA-fusion proteins may have some limitations such as the obvious cross-species difference in FcRn binding [14–16,44,45]. On the other hand, we are not limited to hFcRn transgenic strains, which cannot be used in all disease models.

4.3. Comparison of non-recycling HSA fusions to other half-life extension strategies

We previously compared the pharmacokinetic properties of DARPins fused to unstructured polypeptides and found a linear relationship between the apparent molecular weight and the blood residence time [20]. If the 21 h half-life of HSA in mice were included in the same data plot, it would deviate from the linear fit and the apparent size would appear much larger than its actual size of approximately 65 kDa, despite the fact that it is not bound by the murine FcRn, and would thus not be assumed to participate in endosomal recycling, Moreover, the same half-life around 20 h was also reported for MSA and IgGs in mice that do not express a functional FcRn [11].

In contrast, unstructured polypeptides fused to a DARPin, which show an apparent molecular weight around 300 kDa on gel filtration columns, and hence by far exceed the nominal renal filtration threshold, resulted in half-lives of only around 6 h [20]. Only with an apparent MW of 800–900 kDa, the value of 20 h could be reached [20]. This discrepancy between non-FcRn binding serum albumin variants and unstructured polypeptides suggests that the unstructured polypeptides (and by analogy, other unstructured polymers, such as PEG) are not as strictly excluded by the glomerular filter, but only retarded according to size. An exclusion is possible, but it requires a much higher apparent MW of about 800–900 kDa.

Non-FcRn binding serum albumin variants show half-lives of 20 h in mice, which is significantly longer than those of other proteins of comparable size like antibody fragments [46], single-chain diabody constructs [47,48] or transferrin fusions [49]. These molecules display blood circulation half-lives between one to three hours. Consequently, the *in vivo* binding of serum albumin and IgGs to other receptors such as SPARC, gp60, Fcγ-receptors and the megalin-cubulin complex strongly affects tissue distribution and elimination kinetics [2], even in the absence of FcRn. Unexpectedly, in mice the role of the FcRn in half-life extension of serum albumin is relatively small, at most a factor 1.5, bringing the half-life from 20 h to 30 h. The tissue distribution mediated by other receptors, as well as the reabsorption in the kidney could also explain the herein determined high volumes of distribution, which are in the range of the total calculated body fluid of mice [34] for all tested

HSA constructs. In contrast, the distribution volumes of the recently reported DARPin-polypeptide fusions, which are not bound by specific receptors, are in the range of the total blood volume [20]. The high distribution volume of serum albumin in body tissues serves as a reservoir and, thus, results in comparably long blood circulation half-lives. It would, therefore, be interesting to explore the role of these other serum albumin binding receptors further, both with regard to their influence on half-life, as well as species differences.

4.4. Binding kinetics of different serum albumin variants to human and murine FcRn

To explain the increased half-life of HSA7 in mice when compared to HSA, we measured the affinities for the human and murine FcRn by detailed SPR analyses. Very notable were the low on-rates of 1.1 to 44.2 $\times$ 10^3 $M^{-1}s^{-1}$ of all variants, while typical association rates of protein–protein interactions are in the range of 10^5–10^6 $M^{-1}s^{-1}$ [50]. These low association rates were also described by others [13–16,19,51]. Schmidt et al. [13] proposed a mechanism containing multiple restructuring and binding events, e.g., the movement of an α-helix in DIIIB in HSA13 after initial binding, followed by W53 insertion into its binding pocket. Such a stepwise binding with slow rate-limiting steps could explain the observed slow on-rates, although we have no direct evidence for this mechanism.

HSA7 shows a clearly lower affinity to the murine FcRn than to the human FcRn, and this is visible in the off-rate (Table 1). This difference in affinity between human and murine FcRn is similar to the difference found for another version of HSA with high affinity for the human receptor, HSA^{K573P} [14]. Interestingly, the increased FcRn-affinity of the two published HSA variants, and consequently also the introduced murine FcRn binding and extended half-life in mice, cannot easily be explained from the crystal structures with the human FcRn. One might thus speculate that the introduced amino acid changes rather facilitate the reorientation of DIII and thus act indirectly or mediate long-range effects [14]. It is noteworthy that two different high-affinity versions of HSA (HSA7 and HSA^{K573P}), carrying different amino acid substitutions, bind the murine receptor with a significantly lower affinity than the human one. At the same time, binding of MSA to the murine FcRn can only be described with a different binding model (as exemplified by its requirement for a two-component model (Table 2), correlating with multiple differences in the interacting amino acids between the murine and human FcRn heavy chain homologs [13].

Altogether, this supports the recent finding that serum albumin domains from different species (e.g., DIII from mice or humans) might play very different roles in the interaction with FcRn, again depending on the species of the receptor [16]. Interestingly, murine FcRn-bound HSA7 shows an off-rate comparable to the fast-dissociating murine FcRn/MSA species from the heterogeneous analyte model. MSA binding to murine FcRn, however, displays another slow off-rate. A solved structure of the murine FcRn/MSA complex would be of interest to further elucidate the different binding modes and to explore whether an MSA or HSA derivative with high affinity for murine FcRn, e.g., obtained by *in vitro* evolution, might extend the half-life in mice.

Finally, taking our determined equilibrium dissociation constants together with additional published data [13,14,16], we conclude that low micromolar K_D values are required for FcRn-recycling of serum albumins. This minimal binding is necessary to increase the half-life from 20 to 30 h in mice, and this is the value that MSA has evolved to in mice. Our careful measurements do not confirm the previously reported longer half-life of HSA7 of 67.5 h [13] (Table 2). If this long half-life were correct, we would also have expected a high murine FcRn-affinity of this protein, which we did not observe (Table 1). However, in mice transgenic for the human FcRn, the authors reported a half-life increase of only 1.5 fold from HSA to HSA7, which seems more plausible and better matches with our own data and those reported for another high affinity variant, HSA^{K573P} [14].

4.5. Conclusions

Our data suggest that, since HSA does not bind to the murine FcRn and hence does not reflect the true recycling and biodistribution mechanism of serum albumin in mice, only HSA variants engineered to bind to the murine receptor should be used to investigate the potential for half-life extension, and to improve the pharmacokinetics and efficacy of therapeutic agents under clinically relevant conditions. While one may argue that MSA might be used for such investigations, the use of an HSA variant would allow such a construct to more readily be moved into the clinic.

In conclusion, we designed a novel platform for the fusion, highly efficient production in *P. pastoris*, and preclinical assessment of DARPin-serum albumin constructs in wt mice. Due to its very large distribution volume in different tissues like the lymphatic system and presumably improved tumor penetration, this platform also allows the design of DARPin-agents for novel applications in the future. The strategy can undoubtedly be transferred to other serum albumin fusions of well-behaved proteins.

Declaration of Competing Interest

The authors declare that they have no known competing financial interests or personal relationships that could have appeared to influence the work reported in this paper.

Acknowledgements

The authors would like to thank Valentina Kalichuk, Katja Zerjavic and Ronnie Steiger for their participation in optimizing the serum albumin expression in *P. pastoris* and the purification of the proteins. We would like to thank the Functional Genomics Center Zurich, especially Peter Hunziker, for the N-terminal Edman analysis of different leader sequences and their advice in data interpretation. Furthermore, we would like to thank Simon Jurt (NMR Service, University of Zurich) and Christina Ewald (Cytometry facility, University of Zurich) for their help with NMR data collection and evaluation. This work was supported by Schweizerischer Nationalfonds grant number 31003A-170134 (to U. Z. W.) and 310030_192689 (to A.P.). J.T.A. and J.N. were supported by the Research Council of Norway (Grant no. 314909, 287927 and 274993) and South-Eastern Norway Regional Health Authority (Grant no. 2021069).

Appendix A. Supplementary material

Supplementary data to this article can be found online at https://doi.org/10.1016/j.ejpb.2021.07.011.

References

[1] W.R. Strohl, Fusion proteins for half-life extension of biologics as a strategy to make biobetters, Biodrugs 29 (2015) 215–239.
[2] M. Pyzik, K.M.K. Sand, J.J. Hubbard, J.T. Andersen, I. Sandlie, R.S. Blumberg, The neonatal Fc receptor (FcRn): a misnomer? Front. Immunol. 10 (2019) 1540.
[3] M. Bern, K.M.K. Sand, J. Nilsen, I. Sandlie, J.T. Andersen, The role of albumin receptors in regulation of albumin homeostasis: Implications for drug delivery, J. Control. Release 211 (2015) 144–162.
[4] F.E. Johansen, M. Pekna, I.N. Norderhaug, B. Haneberg, M.A. Hietala, P. Krajci, C. Betsholtz, P. Brandtzaeg, Absence of epithelial immunoglobulin A transport, with increased mucosal leakiness, in polymeric immunoglobulin receptor/secretory component-deficient mice, J. Exp. Med. 190 (1999) 915–922.
[5] R. Kitz, P. Ahrens, S. Zielen, Immunoglobulin levels in bronchoalveolar lavage fluid of children with chronic chest disease, Pediatr. Pulmonol. 29 (2000) 443–451.
[6] M. Dockal, D.C. Carter, F. Rüker, The three recombinant domains of human serum albumin. Structural characterization and ligand binding properties, J. Biol. Chem. 274 (1999) 29303–29310.
[7] E.N. Hoogenboezem, C.L. Duvall, Harnessing albumin as a carrier for cancer therapies, Adv. Drug Deliv. Rev. 130 (2018) 73–89.
[8] Y. Matsumura, H. Maeda, A new concept for macromolecular therapeutics in cancer chemotherapy: mechanism of tumoritropic accumulation of proteins and the antitumor agent SMANCS, Cancer Res. 46 (1986) 6387–6392.

[9] J.T. Isaacs, S.L. Dalrymple, D.M. Rosen, H. Hammers, A. Olsson, T. Leanderson, Anti-cancer potency of tasquinimod is enhanced via albumin-binding facilitating increased uptake in the tumor microenvironment, Oncotarget 5 (2014) 8093–8106.
[10] A. Wunder, U. Müller-Ladner, E.H.K. Stelzer, J. Funk, E. Neumann, G. Stehle, T. Pap, H. Sinn, S. Gay, C. Fiehn, Albumin-based drug delivery as novel therapeutic approach for rheumatoid arthritis, J. Immunol. 170 (2003) 4793–4801.
[11] C. Chaudhury, S. Mehnaz, J.M. Robinson, W.L. Hayton, D.K. Pearl, D.C. Roopenian, C.L. Anderson, The major histocompatibility complex-related Fc receptor for IgG (FcRn) binds albumin and prolongs its lifespan, J. Exp. Med. 197 (2003) 315–322.
[12] V. Oganesyan, M.M. Damschroder, K.E. Cook, Q. Li, C. Gao, H. Wu, W. F. Dall'Acqua, Structural insights into neonatal Fc receptor-based recycling mechanisms, J. Biol. Chem. 289 (2014) 7812–7824.
[13] M. Schmidt, S. Townson, A. Andreucci, B. King, E. Schirmer, A. Murillo, C. Dombrowski, A. Tisdale, P. Lowden, A. Masci, J. Kovalchin, D. Erbe, K. D. Wittrup, E. Furfine, T. Barnes, Crystal structure of an HSA/FcRn complex reveals recycling by competitive mimicry of HSA ligands at a pH-dependent hydrophobic interface, Structure 21 (2013) 1966–1978.
[14] J.T. Andersen, B. Dalhus, D. Viuff, B.T. Ravn, K.S. Gunnarsen, A. Plumridge, K. Bunting, F. Antunes, R. Williamson, S. Athwal, E. Allan, L. Evans, M. Bjørås, S. Kjaerulff, D. Sleep, I. Sandlie, J. Cameron, Extending serum half-life of albumin by engineering FcRn binding, J. Biol. Chem. 289 (2014) 13492–13502.
[15] J.T. Andersen, M.B Daba, G. Berntzen, T.E. Michaelsen, I. Sandlie, Cross-species binding analyses of mouse and human neonatal Fc receptor show dramatic differences in immunoglobulin G and albumin binding, J. Biol. Chem. 285 (2010) 4826–4836.
[16] J. Nilsen, M. Bern, K.M.K. Sand, A. Grevys, B. Dalhus, I. Sandlie, J.T. Andersen, Human and mouse albumin bind their respective neonatal Fc receptors differently, Sci. Rep. 8 (2018) 14648.
[17] A. Plückthun, Designed ankyrin repeat proteins (DARPins): binding proteins for research, diagnostics, and therapy, Annu. Rev. Pharmacol. Toxicol. 55 (2015) 489–511.
[18] C. Zahnd, M. Kawe, M.T. Stumpp, C. de Pasquale, R. Tamaskovic, G. Nagy-Davidescu, B. Dreier, R. Schibli, H.K. Binz, R. Waibel, A. Plückthun, Efficient tumor targeting with high-affinity designed ankyrin repeat proteins: effects of affinity and molecular size, Cancer Res. 70 (2010) 1595–1605.
[19] M. Simon, R. Frey, U. Zangemeister-Wittke, A. Plückthun, Orthogonal assembly of a designed ankyrin repeat protein-cytotoxin conjugate with a clickable serum albumin module for half-life extension, Bioconjug. Chem. 24 (2013) 1955–1966.
[20] F. Brandl, H. Merten, M. Zimmermann, M. Béhé, U. Zangemeister-Wittke, A. Plückthun, Influence of size and charge of unstructured polypeptides on pharmacokinetics and biodistribution of targeted fusion proteins, J. Control. Release 307 (2019) 379–392.
[21] S.B. Petkova, S. Akilesh, T.J. Sproule, G.J. Christianson, H. Al Khabbaz, A. C. Brown, L.G. Presta, Y.G. Meng, D.C. Roopenian, Enhanced half-life of genetically engineered human IgG1 antibodies in a humanized FcRn mouse model: potential application in humorally mediated autoimmune disease, Int. Immunol. 18 (2006) 1759–1769.
[22] J.M. Cregg, J.L. Cereghino, J. Shi, D.R. Higgins, Recombinant protein expression in Pichia pastoris, Mol. Biotechnol. 16 (2000) 23–52.
[23] M. Ahmad, M. Hirz, H. Pichler, H. Schwab, Protein expression in Pichia pastoris: recent achievements and perspectives for heterologous protein production, Appl. Microbiol. Biotechnol. 98 (2014) 5301–5317.
[24] J.M. Cregg, Introduction: distinctions between Pichia pastoris and other expression systems, Methods Mol. Biol. 389 (2007) 1–10.
[25] J.M. Cregg, K.R. Madden, K.J. Barringer, G.P. Thill, C.A. Stillman, Functional characterization of the two alcohol oxidase genes from the yeast Pichia pastoris, Mol. Cell. Biol. 9 (1989) 1316–1323.
[26] R. Couderc, J. Baratti, Oxidation of methanol by the yeast, Pichia pastoris. Purification and properties of the alcohol oxidase, Agric. Biol. Chem. 44 (1980) 2279–2289.
[27] N. Stefan, P. Martin-Killias, S. Wyss-Stoeckle, A. Honegger, U. Zangemeister-Wittke, A. Plückthun, DARPins recognizing the tumor-associated antigen EpCAM selected by phage and ribosome display and engineered for multivalency, J. Mol. Biol. 413 (2011) 826–843.
[28] J.V. Schaefer, A. Plückthun, Engineering aggregation resistance in IgG by two independent mechanisms: lessons from comparison of Pichia pastoris and mammalian cell expression, J. Mol. Biol. 417 (2012) 309–335.
[29] J.T. Andersen, S. Justesen, B. Fleckenstein, T.E. Michaelsen, G. Berntzen, V. E. Kenanova, M.B. Daba, V. Lauvrak, S. Buus, I. Sandlie, Ligand binding and antigenic properties of a human neonatal Fc receptor with mutation of two unpaired cysteine residues, FEBS J. 275 (2008) 4097–4110.
[30] G. Berntzen, E. Lunde, M. Flobakk, J.T. Andersen, V. Lauvrak, I. Sandlie, Prolonged and increased expression of soluble Fc receptors, IgG and a TCR-Ig fusion protein by transiently transfected adherent 293E cells, J. Immunol. Methods 298 (2005) 93–104.
[31] W. Shen, Y. Xue, Y. Liu, C. Kong, X. Wang, M. Huang, M. Cai, X. Zhou, Y. Zhang, M. Zhou, A novel methanol-free Pichia pastoris system for recombinant protein expression, Microb. Cell Fact. 15 (2016) 178.
[32] R.L. Rich, D.G. Myszka, Commercial optical biosensor literature, J. Mol. Recognit. 18 (2005) 1–39.
[33] R.L. Rich, D.G. Myszka, Grading the commercial optical biosensor literature-Class of 2008: 'The Mighty Binders', J. Mol. Recognit. 23 (2010) 1–64.
[34] M.E. Chapman, L. Hu, C.F. Plato, D.E. Kohan, Bioimpedance spectroscopy for the estimation of body fluid volumes in mice, Am. J. Physiol. Renal Physiol. 299 (2010) 280–283.
[35] A.L. Vanz, H. Lunsdorf, A. Adnan, M. Nimtz, C. Gurramkonda, N. Khanna, U. Rinas, Physiological response of Pichia pastoris GS115 to methanol-induced high level production of the Hepatitis B surface antigen: catabolic adaptation, stress responses, and autophagic processes, Microb. Cell Fact. 11 (2012) 103.
[36] F.S. Hartner, A. Glieder, Regulation of methanol utilisation pathway genes in yeasts, Microb. Cell Fact. 5 (2006) 39.
[37] S. Hellwig, F. Emde, N.P. Raven, M. Henke, P. van Der Logt, R. Fischer, Analysis of single-chain antibody production in Pichia pastoris using on-line methanol control in fed-batch and mixed-feed fermentations, Biotechnol. Bioeng. 74 (2001) 344–352.
[38] P. Zhang, W. Zhang, X. Zhou, P. Bai, J.M. Cregg, Y. Zhang, Catabolite repression of Aox in Pichia pastoris is dependent on hexose transporter PpHxt1 and pexophagy, Appl. Environ. Microbiol. 76 (2010) 6108–6118.
[39] S. Sommaruga, A. Lombardi, A. Salvadè, S. Mazzucchelli, F. Corsi, P. Galeffi, P. Tortora, D. Prosperi, Highly efficient production of anti-HER2 scFv antibody variant for targeting breast cancer cells, Appl. Microbiol. Biotechnol. 91 (2011) 613–621.
[40] M. Inan, M.M. Meagher, Non-repressing carbon sources for alcohol oxidase (AOX1) promoter of Pichia pastoris, J. Biosci. Bioeng. 92 (2001) 585–589.
[41] E. Çelik, P. Çalık, S.G. Oliver, Fed-batch methanol feeding strategy for recombinant protein production by Pichia pastoris in the presence of co-substrate sorbitol, Yeast 26 (2009) 473–484.
[42] C. Jungo, J. Schenk, M. Pasquier, I.W. Marison, U. von Stockar, A quantitative analysis of the benefits of mixed feeds of sorbitol and methanol for the production of recombinant avidin with Pichia pastoris, J. Biotechnol. 131 (2007) 57–66.
[43] D. Steiner, P. Forrer, M.T. Stumpp, A. Plückthun, Signal sequences directing cotranslational translocation expand the range of proteins amenable to phage display, Nat. Biotechnol. 24 (2006) 823–831.
[44] J.T. Andersen, J. Cameron, A. Plumridge, L. Evans, D. Sleep, I. Sandlie, Single-chain variable fragment albumin fusions bind the neonatal Fc receptor (FcRn) in a species-dependent manner: implications for in vivo half-life evaluation of albumin fusion therapeutics, J. Biol. Chem. 288 (2013) 24277–24285.
[45] J. Nilsen, I. Sandlie, D.C. Roopenian, J.T. Andersen, Animal models for evaluation of albumin-based therapeutics, Curr. Opin. Chem. Engineering 19 (2018) 68–76.
[46] M. Schlapschy, U. Binder, C. Borger, I. Theobald, K. Wachinger, S. Kisling, D. Haller, A. Skerra, PASylation: a biological alternative to PEGylation for extending the plasma half-life of pharmaceutically active proteins, Protein Eng. Des. Sel. 26 (2013) 489–501.
[47] F. Unverdorben, M. Hutt, O. Seifert, R.E. Kontermann, S. Muyldermans, A Fab-selective immunoglobulin-binding domain from streptococcal Protein G with improved half-life extension properties, PLoS One 10 (2015) e0139838.
[48] F. Unverdorben, F. Richter, M. Hutt, O. Seifert, P. Malinge, N. Fischer, R. E. Kontermann, Pharmacokinetic properties of IgG and various Fc fusion proteins in mice, MAbs 8 (2016) 120–128.
[49] X. Chen, H.F. Lee, J.L. Zaro, W.C. Shen, Effects of receptor binding on plasma half-life of bifunctional transferrin fusion proteins, Mol. Pharm. 8 (2011) 457–465.
[50] H. Nakatanl, H.B. Dunford, Meaning of diffusion-controlled association rate constants in enzymology, J. Phys. Chem. 83 (1979) 2662–2665.
[51] J.T. Andersen, B. Dalhus, J. Cameron, M.B. Daba, A. Plumridge, L. Evans, S. O. Brennan, K.S. Gunnarsen, M. Bjoras, D. Sleep, I. Sandlie, Structure-based mutagenesis reveals the albumin-binding site of the neonatal Fc receptor, Nat. Commun. 3 (2012) 610.
[52] K.K. Schelde, K. Nicholls, F. Dagnaes-Hansen, K. Bunting, H. Rawsthorne, B. Andersen, C.J.A. Finnis, M. Williamson, J. Cameron, K.A. Howard, A new class of recombinant human albumin with multiple surface thiols exhibit stable conjugation, and enhanced FcRn binding and blood circulation, J. Biol. Chem. 294 (2019) 3735–3743.